Sensor and Simulation Notes

Note 381

20 May 1995

Airframes as Antennas

CLEARED
FOR PUBLIC RELEASE
PL/PA 14 JuL 95

Carl E. Baum
Phillips Laboratory

Abstract

In order to lower the frequency of airborne radars down into the region of the dominant resonances of airborne targets, one can use the major dimensions (fuselage and wing) as part of the antenna. In the lower HF band, one can control the excitation of the airframe natural modes using symmetry. In the upper HF band and VHF band one can mount small antennas over these major dimensions to form an array. These two types of antennas can be used for target location and identification, and can be used in a SAR mode to significantly increase the resolution and suppress clutter.

PL 95-0577

Sensor and Simulation Notes

Note 381

20 May 1995

Airframes as Antennas

Carl E. Baum
Phillips Laboratory

Abstract

In order to lower the frequency of airborne radars down into the region of the dominant resonances of airborne targets, one can use the major dimensions (fuselage and wing) as part of the antenna. In the lower HF band, one can control the excitation of the airframe natural modes using symmetry. In the upper HF band and VHF band one can mount small antennas over these major dimensions to form an array. These two types of antennas can be used for target location and identification, and can be used in a SAR mode to significantly increase the resolution and suppress clutter.

1. Introduction

Aircraft have long been used as platforms for various kinds of antennas for various applications (radio, radar, direction finding, etc.). Many of these antennas are small compared to the major aircraft dimensions such as fuselage length and diameter, wing length, etc. These antennas can be electrically large and/or small depending on frequency or pulse characteristics, whether or not they use a metal aircraft skin as a ground plane [3, 4]. This paper considers large antennas (including arrays) which use a large portion or all of the external airframe. These antennas are for operating in the HF or VHF bands, including pulses dominated by these frequencies.

The current discussion concerns the use of such antennas as radars with frequencies considerably below those in common use. By moving the frequency down to the resonant region of airborne targets (aircraft, missiles), one can, in some cases, increase the scattering length (and cross section), thereby allowing one to detect the target at larger ranges [11]. In addition, the target natural frequencies can be used as an identifier via the SEM (similarity expansion method) representation of the scattering [14]. The large dimensions of the target are of the order of a half wavelength in size at the lowest order resonances, thereby indicating the important frequencies. In order to efficiently radiate such frequencies, one needs antennas of similar dimensions (or larger), thereby indicating the use of major portions of the airframe of the airborne antenna platform.

2. Principal Airframe Natural Modes as Antenna Modes

High-frequency band, 3-30 MHz (HF) antennas are an important class of aircraft antennas [12, 13, 16, 19, 20, 23]. Common driving techniques include electric-type (high impedance) "caps" or "probes" on extremities (wing-tips, nose, tail), and magnetic-type (low impedance) shunt-feeds. There may also be special long wires (e.g., from tail cap to fuselage) for the antenna feed. These latter types of feed significantly change the aircraft conducting exterior from an electromagnetic (antenna and scattering) point of view. An example of such lengthy wire feeds is given in fig. 2.1 where the wires run from wing tip to horizontal-stabilizer tip. With sources connecting at either both wing tips or both horizontal-stabilizer tips, the resulting large loop can be driven in push-push or push-pull modes giving a very large antenna. Whether one adopts this approach involves several factors, including aerodynamic ones. Much longer wires are sometimes used for VLF (very-low frequency band, 3-30 kHz) trailing-wire antennas.

As indicated in fig. 2.1, the aircraft exterior (including added wires or other antenna-associated items) is assumed to have an electromagnetic symmetry plane P (the $z = 0$ plane in the usual Cartesian (x, y, z) system) [5, 24]. With the reflection group

$$R_z = \{(1), (R_z)\} \quad , (R_z)^2 = (1) \tag{2.1}$$

(an involution group) and its dyadic (matrix) representation

$$\begin{aligned}
(1) \rightarrow \overleftrightarrow{1} &\equiv \vec{1}_x \vec{1}_x + \vec{1}_y \vec{1}_y + \vec{1}_z \vec{1}_z \equiv \text{identity} \\
(R_z) \rightarrow \overleftrightarrow{R}_z &\equiv \vec{1}_x \vec{1}_x + \vec{1}_y \vec{1}_y - \vec{1}_z \vec{1}_z \\
&= \begin{pmatrix} 1 & 0 & 0 \\ 0 & 1 & 0 \\ 0 & 0 & -1 \end{pmatrix} \equiv \text{reflection through P} \\
\overleftrightarrow{R}_z^2 &= \overleftrightarrow{1}
\end{aligned} \tag{2.2}$$

the electromagnetic fields, currents, etc., can be decomposed into symmetric and antisymmetric parts with the properties

$$\begin{aligned}
\vec{r}_m &\equiv \overleftrightarrow{R}_z \cdot (x, y, -z) \equiv \text{mirror coordinate} \\
\vec{E}_{\substack{sy \\ as}}(\vec{r}_m, t) &= \pm \overleftrightarrow{R}_z \cdot \vec{E}_{\substack{sy \\ as}}(\vec{r}, t) \\
\vec{H}_{\substack{sy \\ as}}(\vec{r}_m, t) &= \mp \overleftrightarrow{R}_z \cdot \vec{H}_{\substack{sy \\ as}}(\vec{r}, t)
\end{aligned} \tag{2.3}$$

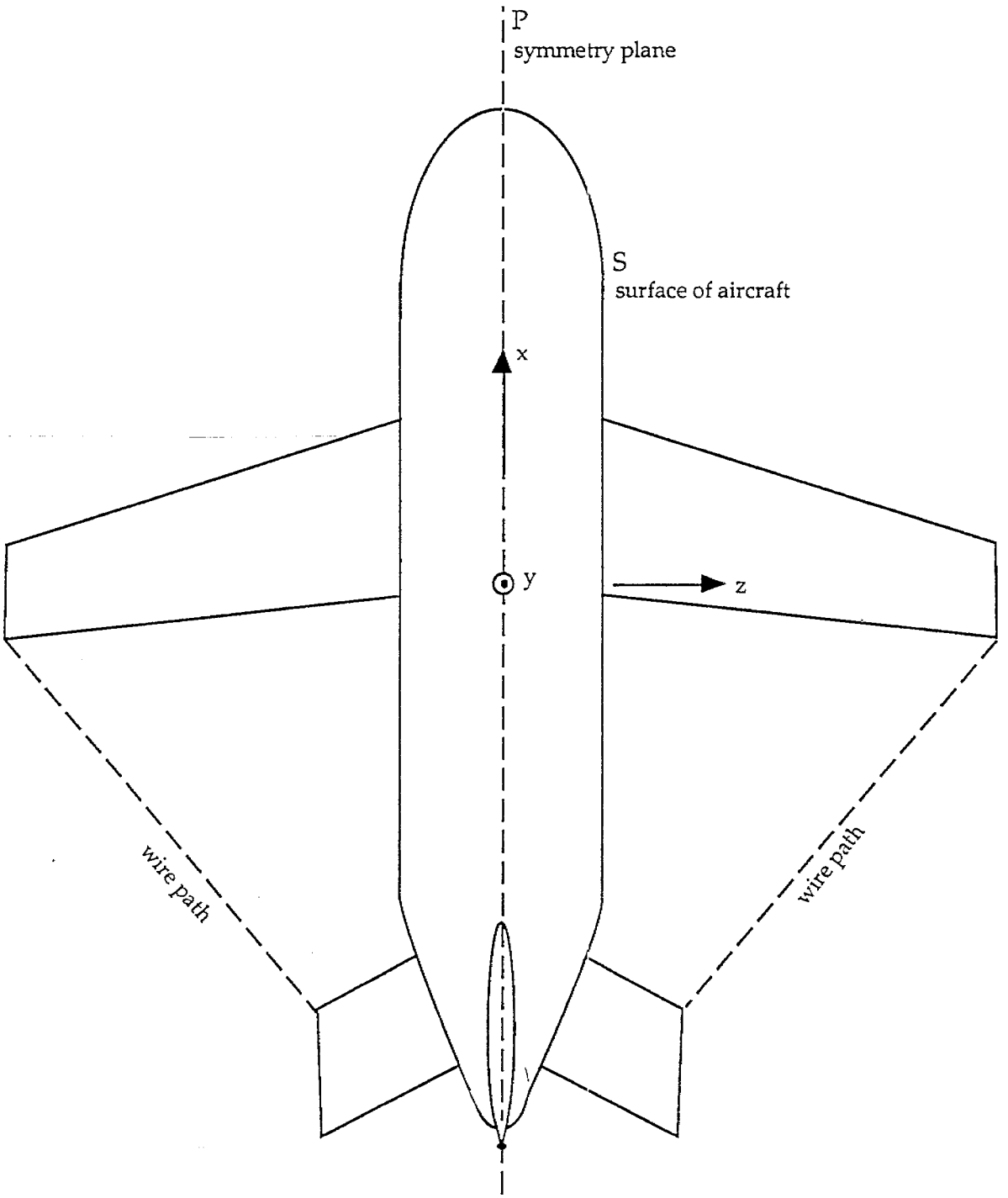

Fig. 2.1. Example Configuration of Wires to Give Large Coupling Loop (Significantly Altering the Natural Modes).

the upper signs applying to the symmetric parts (subscript *sy*) and the lower signs applying to the antisymmetric parts (subscript *as*). This convention also applies to the two decoupled ways or "modes" of operating antennas with this symmetry. Of course, one can use a linear combination of symmetric and antisymmetric modes in both transmission and reception if desired.

The singularity expansion method (SEM) is a useful way of expressing the response (especially transient response) of antennas and scatterers in terms of poles in the complex-frequency plane [8, 14, 17, 18]. Considering the surface current density on an aircraft we can write (antenna in transmission) [7, 18]

$$\tilde{\vec{J}}_s(\vec{r}_s, s) = \tilde{V}(s) \sum_{\alpha} \eta_\alpha \, \vec{j}_{s_\alpha} [s - s_\alpha]^{-1}$$

$$+ \text{ possible entire function}$$

$$\tilde{V}(s) = \text{voltage at antenna gap(s)}$$

$$\eta_\alpha = - \frac{\left\langle \vec{e}_g(\vec{r}_s'); \vec{j}_{s_\alpha}(\vec{r}_s') \right\rangle}{\left\langle \vec{j}_{s_\alpha}(\vec{r}_s'); \frac{\partial}{\partial s} \overleftrightarrow{\tilde{Z}}_t(\vec{r}_s, \vec{r}_s'; s) \Big|_{s = s_\alpha} ; \vec{j}_{s_\alpha}(\vec{r}_s') \right\rangle}$$

$$\equiv \text{coupling coefficient}$$

$$\sim \equiv \text{two-sided Laplace transform (over time } t) \qquad (2.4)$$

$$s \equiv \Omega + j\omega \equiv \text{complex frequency or Laplace-transform variable}$$

$$s_\alpha \equiv \text{natural frequency}$$

$$\vec{j}_{s_\alpha}(\vec{r}_s) \equiv \text{natural mode}$$

$$\vec{r}_s \in S \equiv \text{surface of the aircraft}$$

$$\vec{e}_g(\vec{r}_s') \equiv \text{spatial form of the electric field in the antenna gap(s)}$$

The details need not concern us here, and are found in the references. What is important is the basic form that the poles take, involving natural frequencies (giving damped sinusoids in time domain), natural modes (the spatial distributions over the aircraft), and coupling coefficients (the strengths of the poles due to the excitation $\tilde{V}(s)$ at the antenna port(s)). The form of the coupling coefficient in (2.4) involves symmetric products (integrals over S) and the kernel $\overleftrightarrow{\tilde{Z}}_t$ of the integral equation (e.g., the impedance or E-field kernel) being used. Note that in the antenna case under discussion here the incident field is replaced by the electric field at the antenna gaps. If there is any impedance loading at the antenna gap(s) (source impedance) this also needs to be included as it can affect the natural frequencies and modes.

While (2.4) can be used to calculate the pole parameters, these can also be regarded as experimental observables.

Applying now the reflection symmetry to the natural modes, we have the result that they can be separated into two kinds, symmetric and antisymmetric [1, 2, 6, 10, 17], as

$$\alpha_{\substack{sy \\ as}} \equiv \begin{pmatrix} sy \\ as \end{pmatrix}, \alpha' \Big)$$
$$\vec{j}_{\substack{s_{sy} \\ as', \alpha'}}(\vec{r}_s) = \pm \overleftrightarrow{R}_{s'} \cdot \vec{j}_{\substack{s_{sy} \\ as', \alpha'}}(\vec{r}_s) \tag{2.5}$$

with the associated natural frequencies now being similarly labeled. Note that the natural modes for the surface current density have the same properties as the electric field in (2.3).

Figure 2.2 shows the lowest order natural modes on a simple aircraft structure, these being dominated by the lengths of wing and fuselage being of the order of a half wavelength [1, 6, 17]. The symmetric modes are more complicated due to the interaction of wing and fuselage and the first several of these are illustrated in [9, 19]. The lowest two symmetric modes in fig. 2.2 have the property that one has an important current on the rear part of the fuselage (sy, 1, 1) and the second has an important current on the forward part of the fuselage. The two natural frequencies can be close to each other depending on how close the geometry approximates a symmetrical cross (with a second symmetry plane perpendicular to the x axis).

One can position antenna gaps in shunt feeds as indicated in fig. 2.3 to excite these principal natural modes (and higher-order ones as well). In this example, there are gaps fore and aft of the two wing roots. By appropriate excitations of these four antenna gaps, one can preferentially excite particular modes. Note the possible use of dielectric to make the loop areas aerodynamically part of the wing surfaces.

The simplest case is the antisymmetric mode (as, 1) in fig. 2.2C, this being the half-wave resonance of the wing with no net current through any cross section (plane perpendicular to the x axis) of the fuselage. By using equal but opposite polarities on port and starboard antenna gaps (push-pull configuration) the gap electric fields are antisymmetric as described in (2.3). The relative amplitudes of the fore and aft gap voltages can also be adjusted if desired. The radiation pattern of this mode is approximately that of an electric dipole with a maximum on P (the $z = 0$ plane) in the far field. As a down-looking radar, this then is appropriate for searching for targets fore and aft, for which the polarization is horizontal.

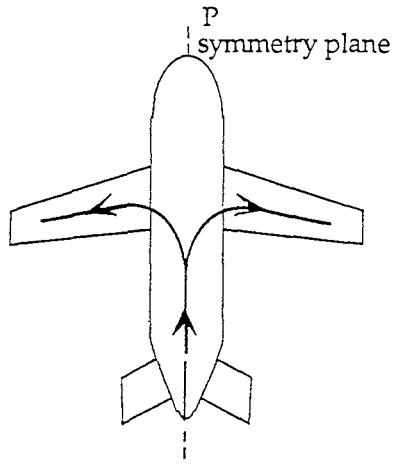

A. *sy*, 1, 1 mode

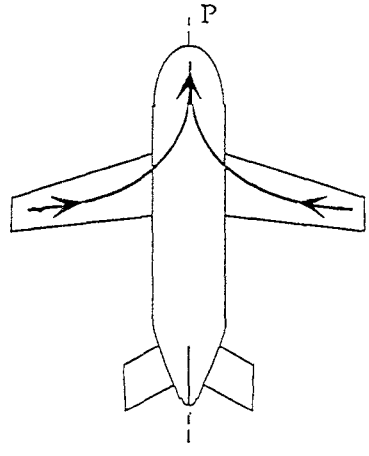

B. *sy*, 1, 2 mode

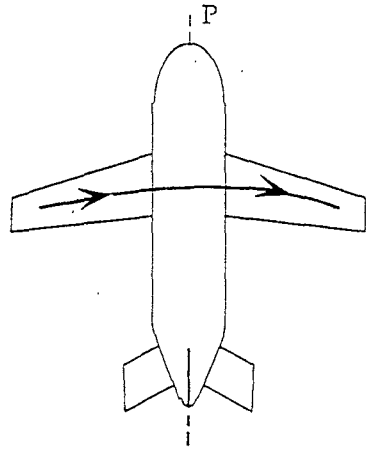

C. *as*, 1 mode

Fig. 2.2. Principal Natural Modes of an Aircraft: Arrows on Current Paths Indicate Current Directions.

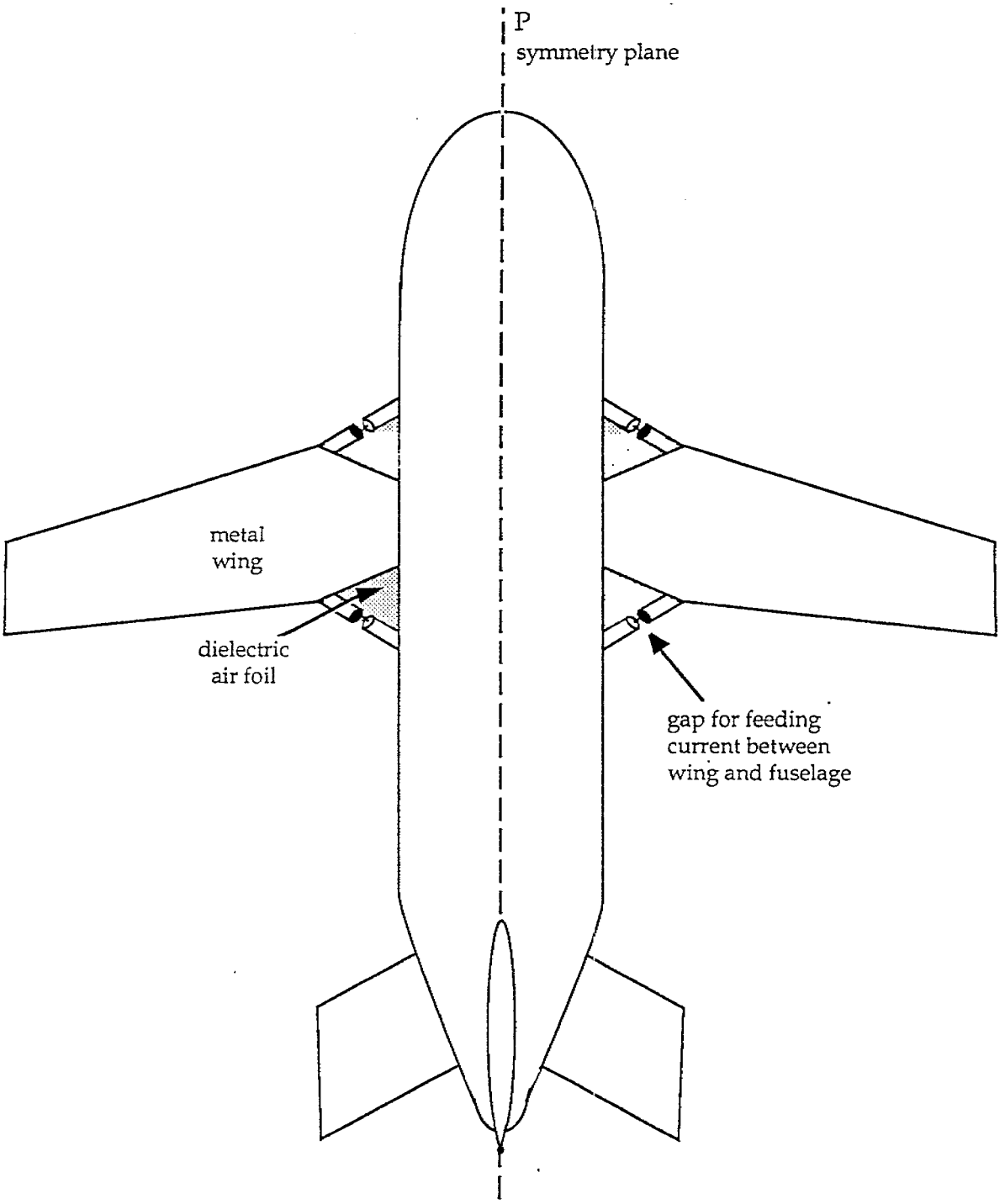

Fig. 2.3. Wing-Root Inductive Couplers: Push-Push for Symmetric Modes and Push-Pull for Antisymmetric Modes.

For symmetric excitation, one uses the same polarity with equal excitations on port and starboard to give a symmetric gap electric field as in (2.3). This still leaves the relative amplitudes (and phases) of the fore and aft gap voltages to be considered. The two symmetric modes can roughly be considered as being fore (sy, 1, 2) and aft (sy, 1, 1) modes in figs. 2.2B and 2.2A respectively. By emphasizing the fore gap voltages where the fore mode is stronger one expects to more strongly excite the fore mode, and conversely for the aft mode. By appropriate combinations of fore and aft voltages one might even approximately separate the two modes. Since these two modes have different natural frequencies one can use these modes in combination for broad banding the transmitting antenna. Both of these modes will have electric-dipole-like characteristics with dipole moments parallel to P and approximately parallel to the x axis. As a downlooking radar, this is appropriate for searching for targets abeam, for which the polarization is again horizontal.

3. Large Arrays on Airframe

As one goes higher in frequency, the fuselage and wing lengths become many wavelengths in length, and the first few natural modes are not adequate to describe the response. There is, however, some benefit to having these dimensions several wavelengths since one can now consider arrays of antennas mounted over the lengths of the fuselage and/or wing to obtain a narrower antenna beam (greater directivity) for better locating a target and for better clutter suppression. While the antennas of Section 2 are appropriate for the lower part of the HF band, the arrays considered here are appropriate for the upper part of the HF band and for the VHF (very-high frequency, 30-300 MHz) band. Of course, one can go to even higher frequencies (as is typically done with aircraft radars), but these arrays are small compared to the fuselage and wing lengths. Furthermore, the frequencies of interest for our purposes here are in the resonant region of the targets of interest for which half wavelengths are of the order of (or not too much smaller than) the target major dimensions.

Consider now the kind of antenna elements one might wish to have in the array. As discussed in [4], if one wishes to transmit or receive in a direction normal to a conducting surface, a magnetic dipole is preferable to an electric dipole. Another advantage is that, if the individual antennas (array elements) are electrically small, the magnetic dipoles are constructed as loops which have a low input impedance in this frequency region. So let us consider arrays of such loops mounted on the aircraft skin with magnetic moments $\vec{m}$ parallel to the aircraft skin (and including the loop images inside the aircraft). Note, however, that one can also use electric dipoles with dipole moments perpendicular to the skin, or even combinations of electric and magnetic dipoles.

Figure 3.1 illustrates what an array of such antennas might look like for a down-looking radar, for which the antennas are mounted under the fuselage and wing. The antennas under the fuselage can be contained in a dielectric fairing running the length of the fuselage. This is a keel-like structure and the associated antennas can be referred to as keel antennas which are part of the keel array. This keel array can be used to scan fore and aft with a beam width of the order λ/ℓ (in radians) where λ is the wavelength and ℓ the length of the array [15]. Under the wings, the loops can also be enclosed in dielectric pylons. This wing array might also include antennas in the currently popular winglets at the wing tips. Such an array can scan from side to side with similar angular resolution. Between the two arrays, one can scan in two angles, the third coordinate, range, being given by the usual time delay.

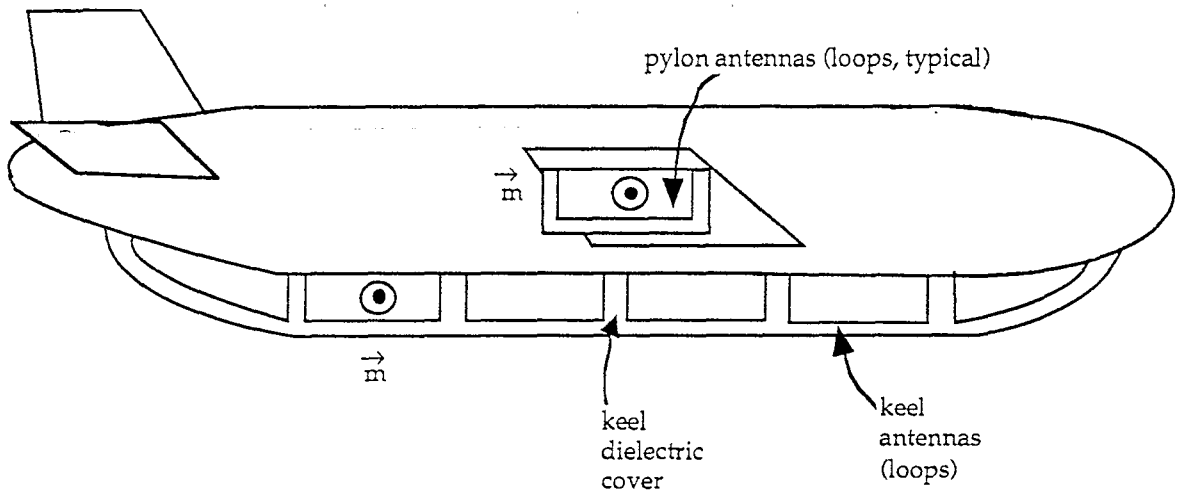

A. side view

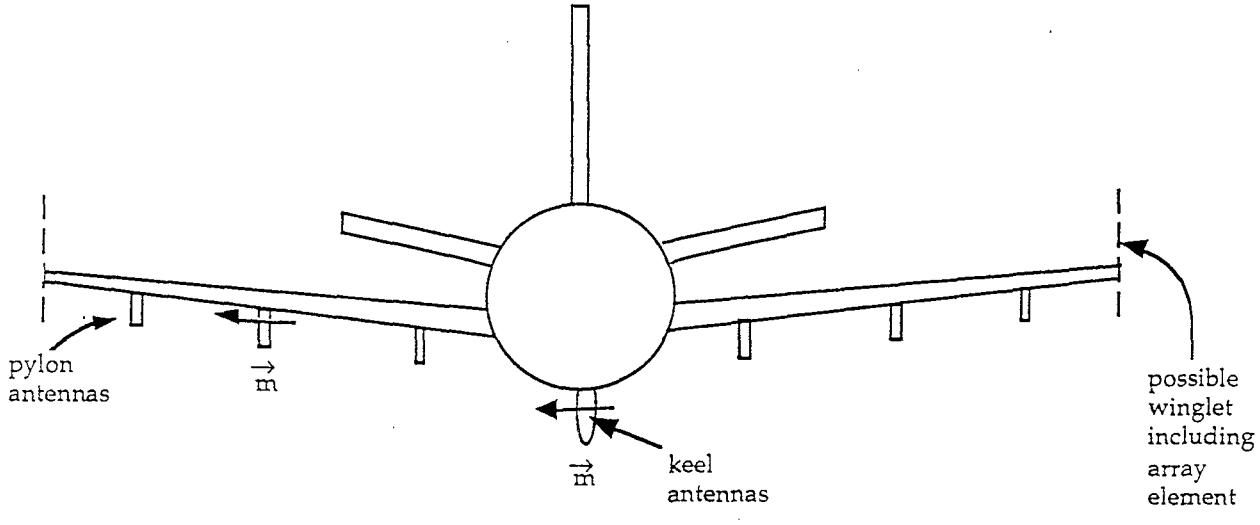

B. front view

Fig. 3.1. Array of Magnetic Dipoles Under Fuselage and Wing.

The orientation of the magnetic dipole moments $\vec{m}$, as indicated in fig. 3.1, is perpendicular to the direction of motion of the aircraft (relative to the air) for aerodynamic convenience. The planes of the loops are then parallel to the air flow. For the chosen antenna locations the magnetic moments are approximately perpendicular to P (and, except for phasing (or timing) symmetric with respect to P). For targets near P and near the earth surface the incident electric field is parallel to P and perpendicular to a radius vector from the array platform. In radar parlance this is referred to as vertical polarization. Note, however, that directly under the array the incident electric field is parallel to P and to the earth surface (i.e., strictly horizontal). Abeam and below the aircraft the incident electric field is horizontally polarized (and parallel to P). For more general target locations the polarizations of the incident field is in general a combination of both polarizations. Polarization at the target is important and one would like to have the incident electric field as nearly as practical parallel to the conductors of greatest length (e.g., fuselage and/or wing of the target). By reorienting the magnetic dipole moments one can obtain other polarizations but at an increase in mechanical complexity (e.g., by allowing air to flow through loops oriented with $\vec{m}$ parallel to the air flow).

The location of the antennas in fig. 3.1, has been selected on the assumption that one is interested in a down-looking radar. If one is interested in searching for targets at the same or higher altitudes compared to the radar, one might choose other locations for the antennas. For example, the keel antennas might be moved to the sides or top of the fuselage.

4. Radar Applications

Let us now consider how these antennas might functions part of a radar. As in fig. 4.1, the radar platform is assumed flying at some altitude h_p with velocity $\vec{v}_p$, typically parallel to the local earth surface underneath. Similarly the target is assumed flying at altitude h_t with velocity $\vec{v}_t$. The distance between the projections of the platform and target on the earth surface (assumed approximately level) is d, and their relative altitude is $h_p - h_t$, giving a relative separation

$$r = \left[d^2 + \left(h_p - h_t \right)^2 \right]^{\frac{1}{2}} \tag{4.1}$$

There is also an angle of elevation of the platform above the target as

$$\psi = \arctan\left(\frac{h_p - h_t}{d} \right) = \arcsin\left(\frac{h_p - h_t}{r} \right) = \arccos\left(\frac{d}{r} \right) \tag{4.2}$$

The two velocities, while assumed for level flight, need not be parallel to the page.

By the scattered signal returning on the direct path (P_1 in both directions) one readily determines r. Furthermore, through the use of Doppler techniques, or equivalently the time of return of subsequent pulses, we have dr/dt which can be interpreted as

$$\begin{aligned} \frac{dr}{dt} &= \vec{1}_r \cdot [\vec{v}_t - \vec{v}_p] \\ \vec{1}_r &\equiv \frac{\vec{r}_t - \vec{r}_p}{r} \\ r &\equiv | \vec{r}_t - \vec{r}_p | \\ \vec{r}_t &\equiv \text{target position} \\ \vec{r}_p &\equiv \text{platform position} \end{aligned} \tag{4.3}$$

From the ground return (from non-moving features on the earth surface) or various other techniques the platform velocity $\vec{v}_p$ can be determined. If one has sufficient angular resolution and observes the target for sufficient time, one can determine the cross range velocity. Note that here, down range and cross range refer to a coordinate (inertial reference frame) based on the radar platform, so that the velocity components are components of $\vec{v}_t - \vec{v}_p$.

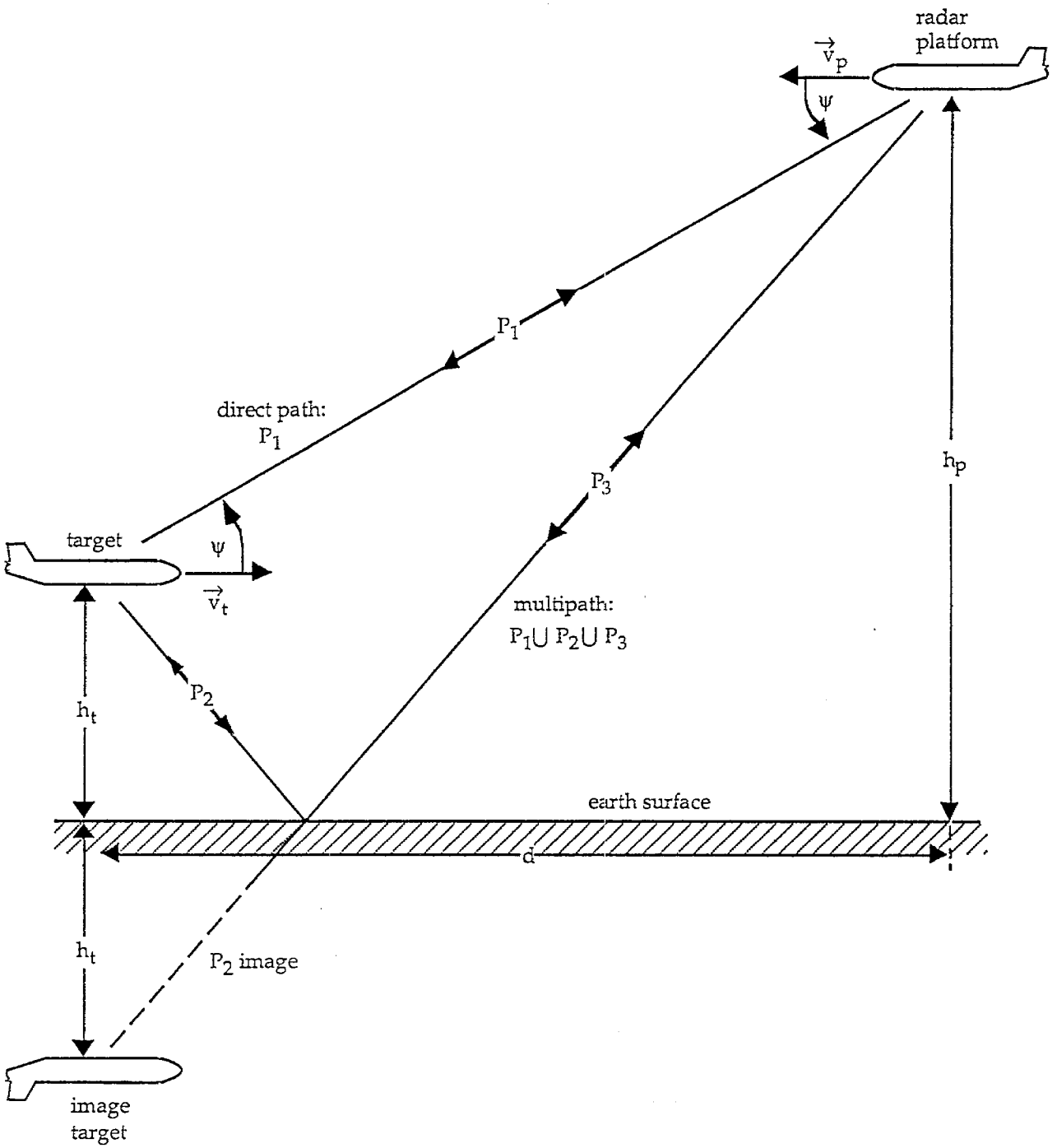

Fig. 4.1. Radar Platform and Target

The second signal to return from the target to the radar platform is via the multipath as illustrated in fig. 4.1. The multipath can be traversed in two directions: P_1 (radar to target), followed by P_2 (target to earth surface), followed by P_3 (earth surface to radar), or in the reverse direction around the loop (i.e., P_3, then P_2, then P_1). Assuming reciprocity, the contributions of the waves propagating around this multipath are equal for both directions, thereby doubling the signal from what one would calculate from a single bistatic scattering at the target and the earth surface. If the scattering from the earth surface is not too lossy (e.g., sea water) and the bistatic scattering at the target is comparable to the monostatic scattering, this multipath signal can even be larger than the direct-path signal. Consider the various path lengths

$$\begin{aligned} \ell_n &\equiv \text{length of } P_n \\ \ell_1 &= r \\ 2\ell_1 &= 2r \equiv \text{path length for direct signal} \\ \sum_{n=1}^{3} \ell_n &\equiv \text{path length for multipath signal} \end{aligned} \tag{4.4}$$

Assume a low-flying target such that

$$h_t << h_p \tag{4.5}$$

making P_3 approximately parallel to P_1. Then $\ell_2 + \ell_3$ can be estimated (being also the distance from the radar to the image target) via

$$\begin{aligned} \ell_2 + \ell_3 &= \left[\left(h_p + h_t \right)^2 + d^2 \right]^{\frac{1}{2}} \\ &= \left[\left(h_p - h_t \right)^2 + 4h_p h_t + d^2 \right]^{\frac{1}{2}} \\ &= \left[\ell_1^2 + 4h_p h_t \right]^{\frac{1}{2}} \\ &= \ell_1 \left[1 + \frac{2h_p h_t}{\ell_1^2} + O\left(\left(\frac{h_p h_t}{\ell_1^2} \right)^2 \right) \right] \\ &\qquad \text{as } \frac{h_p h_t}{\ell_1^2} \to 0 \end{aligned} \tag{4.6}$$

The difference in path lengths for multipath and direct is then

$$\Delta\ell_m = [\ell_1 + \ell_2 + \ell_3] - 2\ell_1$$

$$\frac{\Delta\ell_m}{\ell_1} = \frac{2h_p\, h_t}{\ell_1^2} + O\left(\left(\frac{h_p\, h_t}{\ell_1^2}\right)^2\right) \quad \text{as} \quad \frac{h_p\, h_t}{\ell_1^2} \to 0 \tag{4.7}$$

With ℓ_1, $\Delta\ell_m$, and h_p available from measurement we have

$$h_t \simeq \frac{\ell_1\, \Delta\ell_m}{2h_p} \simeq \frac{\Delta\ell_m}{2\sin(\psi)} \tag{4.8}$$

as an estimate of the target altitude. Of course, one need not use the approximation in (4.6), but can solve the equations for h_t.

After the multipath signal discussed above, there is the signal from the wave propagation from the radar via P_3 and P_2 to the target and returning via P_2 and P_3. The path length is the same as the round trip path between the radar and the target image. This has the additional path length over the direct path as

$$\Delta\ell_i = 2[\ell_2 + \ell_3] - 2\ell_1$$

$$\frac{\Delta\ell_i}{\ell_1} = \frac{4h_p\, h_t}{\ell_1^2} + O\left(\left(\frac{h_p\, h_t}{\ell_1^2}\right)^2\right) \text{ as } \frac{h_p\, h_t}{\ell_1^2} \to 0 \tag{4.9}$$

$$\simeq 2\frac{\Delta\ell_m}{\ell_1}$$

so the time intervals between direct and multipath, and between multipath and image are about the same, further aiding in the determination of the target altitude.

Besides h_t, we would also like to know the horizontal range to the target. From (4.1) we directly have

$$d = \left[r^2 - \left(h_p - h_t\right)^2\right]^{\frac{1}{2}} \tag{4.10}$$

for small h_t, this reduces to

$$d = \left[r^2 - h_p^2\right]^{\frac{1}{2}} \simeq r\,\cos(\psi) \tag{4.11}$$

One of the limitations of radars at these frequencies (given the size of aircraft platforms) is the directivity of the radar because of the frequencies (LF and VLF) proposed for use. As discussed above, various parameters can be determined from time of arrival of the radar return signals. However, the cross range parameters (azimuthal angle and relative azimuthal velocity) are more difficult to obtain if one has a broad-beam radar.

Perhaps a modern concept, namely SAR (synthetic aperture radar), can be of help [21, 22]. Again referring to fig. 4.1, assume for the moment that the target is stationary. As the radar aircraft moves at velocity $\vec{v}_p$ (assumed constant for simplicity, but not necessary) and continues to emit and receive radar pulses, if the data for each pulse is stored and compared from pulse to pulse, the effect that can be achieved is to have the size of the radar antenna be increased to

$$\ell_s = |\vec{v}_p|\,\Delta t_s \tag{4.12}$$
Δt_s = length of time recordings are taken (over many radar pulses)

where the subscript s refers to SAR. The effective beamwidth is then given (in radians) by [22]

$$\beta_s \simeq \frac{\lambda}{2\,\ell_s} = \frac{\lambda}{2\,|\vec{v}_p|\,\Delta t_s} \tag{4.13}$$

the factor of 2 coming from the phase difference in the round-trip path. By flying fast enough ($\vec{v}_p$) for enough time (Δt_s) quite good resolution can be achieved. Even with long wavelengths (tens of meters at HF) the aircraft can move to give hundreds of meters or even kilometers for ℓ_s.

With the target moving at velocity $\vec{v}_t$, it is, of course, the relative velocity $\vec{v}_p - \vec{v}_t$ that one should use in the formulas. The reader can note that ISAR (inverse SAR) is sometimes used to designate the case in which the radar is stationary and the target is moving. Our present situation is, however, more general in that both move. Of course, using special-relativity concepts one can regard the target as stationary (inertial reference frame) and the radar as moving, or conversely. Actually, the target motion (relative to the local earth) can be used to advantage for clutter suppression. As one focuses the SAR processing on the moving target the returns from earth-surface perturbations (hills, waves, etc.) are averaged out (or effectively defocused).

away from the radar platform, then one can orient the direction of platform flight so that $\vec{v}_p$ has a significant component perpendicular to this direction, giving the common configuration of a side-looking SAR. It may then be useful to vary the direction of flight of the radar to obtain various value of $\vec{v}_p$.

5. Concluding Remarks

This paper has presented two general concepts for airframe-based radar antennas for HF and VHF bands. By going to these lower frequencies (lower than commonly used aircraft radar frequencies) one can make half wavelengths of the order of major target dimensions. This can increase the target scattering (depending on target), and can be used to identify the target based on its aspect-independent natural frequencies as described in the SEM, provided there are sufficient frequencies (sufficient bandwidth) in the radar pulse.

In order to achieve cross-range resolution and suppress ground clutter, one can use SAR techniques. The SAR portion is not for identification, but location. Note that we are not looking for resolution sufficient to resolve small geometric features of the target sufficient to produce an identifiable image. We are looking for enough resolution to pinpoint the target location (average), especially in cross range. The SAR technique allows one to achieve this resolution, even with these relatively long wavelengths. Note that SAR is not the only way, in principle, to achieve this resolution. With two radar aircraft one can also use bistatic techniques.

References

1. T. T. Crow, C. D. Taylor, and M. Kumbale, The Singularity Expansion Method Applied To Perpendicular Crossed Wires Over a Perfectly Conducting Ground Plane, Sensor and Simulation Note 258, June 1979.

2. D. V. Giri and C. E. Baum, Airborne Platform for Measurement of Transient or Broadband CW Electromagnetic Fields, Sensor and Simulation Note 284, May 1984, and Proc. AICWEMC, Bangalore, India, Nov. 1985, pp. 79-82, and Electromagnetics, 1989, pp. 69-84.

3. C. E. Baum, Low-Frequency Compensated TEM Horn, Sensor and Simulation Note 377, January 1995.

4. C. E. Baum, Variations on the Impulse-Radiating-Antenna Theme, Sensor and Simulation Note 378, February 1995.

5. C. E. Baum, Interaction of Electromagnetic Fields With an Object Which Has an Electromagnetic Symmetry Plane, Interaction Note 63, March 1971.

6. T. T. Crow, B. D. Graves, and C. D. Taylor, The Singularity Expansion Method as Applied to Perpendicular Crossed Cylinders in Free Space, Interaction Note 161, October 1973, and IEEE Trans. Antennas and Propagation, 1975, pp. 540-546.

7. C. E. Baum, Single Port Equivalent Circuits for Antennas and Scatterers, Interaction Note 295, March 1976.

8. C. E. Baum, Emerging Technology for Transient and Broad-Band Analysis and Synthesis of Antennas and Scatterers, Interaction Note 300, November 1976, and Proc. IEEE, 1976, pp. 1598-1616.

9. G. Bedrosian, Stick-Model Characterization of the Natural Frequencies and Natural Modes of the Aircraft, Interaction Note 326, September 1977.

10. C. E. Baum, A Priori Application of Results of Electromagnetic Theory to the Analysis of Electromagnetic Interaction Data, Interaction Note 444, February 1985, and Radio Science, 1987, pp. 1127-1136.

11. C. E. Baum, Transient Scattering Length and Cross Section, Interaction Note 484, April 1991.

12. I. Carswell, Current Distribution on Wing-Cap and Tail-Cap Antennas, IRE Trans. Antennas and Propagation, 1955, pp. 207-212.

13. R. L. Tanner, Shunt and Notch-Fed HF Aircraft Antennas, IRE Trans. Antennas and Propagation, 1958, pp. 35-43.

14. C. E. Baum, E. J. Rothwell, K.-M. Chen, and D. P. Nyquist, The Singularity Expansion Method and Its Application to Target Identification, Proc. IEEE, 1991, pp. 1481-1492.

15. H. Jasik, Fundamentals of Antennas, ch. 2, in H. Jasik (ed.), *Antenna Engineering Handbook*, McGraw Hill, 1961.

16. J. T. Bolljahn and J. V. N Granger, Aircraft Antennas, ch. 27, in H. Jasik (ed.), *Antenna Engineering Handbook*, McGraw Hill, 1961.

17. C. E. Baum, The Singularity Expansion Method, ch. 3, pp. 129-179, in L. B. Felsen (ed.), *Transient Electromagnetic Fields*, Springer-Verlag, 1976.

18. C. E. Baum, Toward an Engineering Theory of Electromagnetic Scattering: The Singularity and Eigenmode Expansion Methods, ch. 15, pp. 571-651, in P. L. E. Uslenghi (ed.), *Electromagnetic Scattering*, Academic Press, 1978.

19. K. S. H. Lee (ed.), *EMP Interaction: Principles, Techniques, and Reference Data*, Hemisphere Publishing Corp. (Taylor & Francis), 1986.

20. K. S. H. Lee, Antenna Response to Electromagnetic Pulses, ch. 30, in Y. T. Lo and S. W. Lee (eds.) *Antenna Handbook*, Van Nostrand Reinhold, 1988.

21. J. P. Fitch, *Synthetic Aperture Radar*, Springer-Verlag, 1988.

22. L. J. Cutrona, Synthetic Aperture Radar, ch. 21, in M Skolnik (ed.), *Radar Handbook, 2nd Ed.*, McGraw Hill, 1990.

23. W. P. Allen, Jr., and C. E. Ryan, Jr., Aircraft Antennas, ch. 27, in R. C. Johnson (ed.) *Antenna Engineering Handbook, 3rd Ed.*, McGraw Hill, 1993.

24. C. E. Baum and H. N. Kritikos, Symmetry in Electromagnetics, ch. 1, pp. 1-90, in C. E. Baum and H. N. Kritikos (eds.), *Electromagnetic Symmetry*, Taylor & Francis, 1995.